Deviation from the direction of motion across gaits in a hexapodal robot

Zijie Niu
Northwest Agriculture and Forestry University, Yangling, China
Aiwen Zhan
Institutes of Technology of South China, Guangdong, UK, and
Yongjie Cui
Northwest Agriculture and Forestry University, Yangling, China

Abstract

Purpose – The purpose of this study is to test a chassis robot on rugged road cargo handling.

Design/methodology/approach – Attitude solution of D-H series robot gyroscope speed and acceleration sensor.

Findings – In identical experimental environments, hexapodal robots experience smaller deviations when using a four-footed propulsive gait from a typical three-footed gait for forward motion; for the same distance but at different speeds, the deviation basically keeps itself within the same range when the robot advances forward with four-foot propulsive gait; because the foot slide in the three-footed gait sometimes experiences frictions, the robot exhibits a large gap in directional deviations in different courses during motion; for motion using a four-footed propulsive gait, there are minor directional deviations of hexapodal robots resulting from experimental errors, which can be reduced through optimizing mechanical structures.

Originality/value – Planning different gaits can solve problems existing in some typical gaits. This article has put forward a gait planning method for hexapodal robots moving forward with diverse gaits as a redundant multifreedom structure. Subsequent research can combine a multiparallel-legged structure to analyze kinematics, optimize the robot's mechanical structure and carry out in-depth research of hexapod robot gaits.

Keywords Kinematic analysis, Four-footed propulsive gait, Gait planning, Hexapod robot, Three-footed gait

Paper type Research paper

1. Introduction

With the development of science and technology, and the continuous exploration of nature, humankind has uncovered and developed dangerous working environments (earthquake damaged areas, deep seas, collapsed mines, ships and bridges). Robots are the prime choice for probing such environments (Agheli and Nestinger, 2016; Arevalo *et al.*, 2014; Zhong *et al.*, 2017). Compared with wheeled mobile robots (Song *et al.*, 2016; Grand *et al.*, 2004) and tracked robots (Fujita and Tsuchiya, 2015; Lee *et al.*, 2003), legged robots are more stable and maneuverable in rugged areas (Zhong *et al.*, 2016; Li *et al.*, 2017). However, hexapodal robots typically suffer from redundant drive systems (Yang and Feng, 2014) and complicated mechanical structures; hence, their movement control is tedious. Targeting the movement of hexapodal robots in rugged area, Zhong *et al.* (2017) used central pattern generator-based network control to plan gaits that produced steady movement. Zhao *et al.* (2018) put forward obstacle avoidance and motion planning schemes that permit hexapod robots to navigate around large obstacles. There are also a lot of researches on gait and energy efficiency of hexapod robot. Armada *et al.* (2005) used crawling robots in marine industry. Grieco *et al.* (1998) used hexapod robot for high-altitude work. Montes *et al.* (2017) used hexapod robots in mine clearance operations. Gonzalez de Santos *et al.* (2009) proposed the energy minimization model of hexapod robot. Guardabrazo and Gonzalez de Santos (2004) established an energy consumption model of a crawling robot and optimized it.

Motion control tactics can be simplified when a hexapod robot moves across normal terrain; for such areas, researchers have planned three-footed (Yin, 2014), four-footed (Ding, 2016) and turning (Gao *et al.*, 2015) gaits, which experience motion deviation during operation. To solve the problem of deviation when hexapodal robots move with these gaits, Chen *et al.* (2014) proposed a closed-circuit control algorithm to resolve deviations of semicircle rigid foot positions in rugged area, ignoring flat situations; Zhang *et al.* (2016) considered that when gait distance coincides with certain motion terms in a tripod-based gait, the robot's motion is static and steady; inspired by the biological behaviors of ants, Zhu *et al.* (2017) put forth random gait turning and radius correction algorithms

The current issue and full text archive of this journal is available on Emerald Insight at: **https://www.emerald.com/insight/0143-991X.htm**

Industrial Robot: the international journal of robotics research and application
47/3 (2020) 325–333
 [ISSN 0143-991X]
[DOI 10.1108/IR-03-2019-0054]

Funding: This work was supported in part by the Basic Research Plan of Natural Science of Shaanxi Province 2019JQ-305) and National Key Research and Development Project (2019YFD1002400).

Received 16 March 2019
Revised 21 October 2019
18 November 2019
16 December 2019
30 December 2019
Accepted 6 January 2020

for hexapodal robots, which corrected turning deviation for random gaits but failed to examine straight-line gaits.

In recent years, scholars have done a lot of research on the mechanical analysis, gait planning and adaptive control of complex terrain of hexapod robot. A static and stable terrain adaptive strategy for hexapod walking robot is proposed by Castro and Castaneda (2019). The research on the foot force distribution, energy consumption and dynamic stability of hexapod robot in the process of crab walking was proposed by Abhijit *et al.* (2018). Toward dynamic alternating tripod trotting of a pony-sized hexapod robot for disaster rescuing based on multi-modal impedance control was proposed by Sun *et al.* (2018). Locomotion control and gait planning of a novel hexapod robot using biomimetic neurons was proposed by Zhong *et al.* (2018). A study of arbitrary gait pattern generation for turning of a bio-inspired hexapod robot was proposed by Zhu *et al.* (2017).

At present, GPS and other devices can ensure the navigation accuracy of the robot in the process of walking. However, when the error of free gait is caused by rough road or load, different gaits should be used to compensate the walking error. This paper first describes the deviation problems in existing hexapodal robots that move with a typical three-footed gait across flat areas, analyzing the practical reasons for this deviation; second, our study combines the factors that bring about deviations in three-footed gaits based on the foundation of the robot's foot-side kinematic to plan a four-footed propulsive gait; finally, these two gaits are compared experimentally, proving that a planned four-footed propulsive gait exerts less deviation than the typical three-footed gait from the direction of motion.

2. Kinematic analysis

2.1 Direct kinematic analysis of a single foot with three degrees of freedom

The robot in this article has six identically sized feet distributed symmetrically on both sides of its body. The structure of the feet is shown in Figure 1. Each foot is equipped with root, hip and knee joints; the axes of the root and knee joints remain perpendicular. We use a Denavit–Hartenberg (DH) approach to establish a joint's coordinate system (Zhuang *et al.*, 2017; Hasnaa and Mohammed, 2017; Grzelczyk *et al.*, 2017) relative to the hexapod robot's foot, where $\{O_b - X_bY_bZ_b\}$ is regarded as the coordinate system of the hexapod robot's body, and the original position in the coordinate system of body is located in the superficial center of the body; $\{O_{i0} - X_{i0}Y_{i0}Z_{i0}\}$ is the coordinate system of the knee joints relative to foot i; $\{O_{i1} - X_{i1}Y_{i1}Z_{i1}\}$ is the coordinate system of the hip joints relative to foot i; $\{O_{i2} - X_{i2}Y_{i2}Z_{i2}\}$ is the coordinate system of the knee joints relative to foot i; and $\{O_{i3} - X_{i3}Y_{i3}Z_{i3}\}$ denotes the foot-side coordinate system related to foot i. The establishment of coordinate systems adheres to the DH approach to formulating rules and conforms to the right-hand (spiral) rule. Single-foot DH parameters and joint variables are displayed in Table I.

The DH approach is used to establish the kinematic equation for i as follows:

$$ {}^{0}T_{i3} = {}^{0}A_{i1}\,{}^{1}A_{i2}\,{}^{2}A_{i3} \tag{1} $$

${}^{j-1}A_{ij}$ (j = 1, 2, 3) can be treated as a transformation matrix between the $j-1$ and j coordinate systems:

Figure 1 Establishment of a single-foot coordinate system based on a DH approach

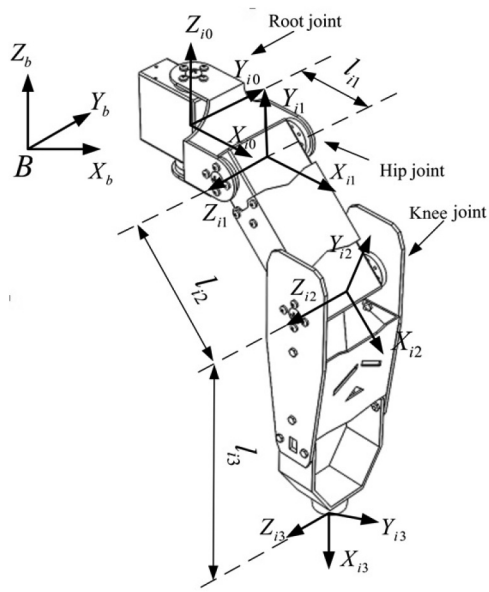

Table I DH parameter and joint variables

j	θ_{ij}	d_{ij}	a_{ij}	α_{ij}	Range of values of θ_{ij}
1	θ_{i1}	0	l_{i1}	$\frac{\pi}{2}$	$\theta_{i1} \in \left[-\frac{\pi}{2}, \frac{\pi}{2}\right]$
2	θ_{i2}	0	l_{i2}	0	$\theta_{i2} \in \left[-\frac{\pi}{2}, \frac{\pi}{2}\right]$
3	θ_{i3}	0	l_{i3}	0	$\theta_{i3} \in [-\pi, 0]$

$$ {}^{j1}A_{ij} = Rot(Z_{i(j-1)}, \theta_{ij})\,Trans(a_{ij}, 0, d_{ij})\,Rot(X_{ij}, \alpha_{ij}) $$
$$ = \begin{bmatrix} c\theta_{ij} & -s\theta_{ij}c\alpha_{ij} & s\theta_{ij}s\alpha_{ij} & a_{ij}c\theta_{ij} \\ s\theta_{ij} & c\theta_{ij}c\alpha_{ij} & -c\theta_{ij}s\alpha_{ij} & a_{ij}s\theta_{ij} \\ 0 & s\alpha_{ij} & c\alpha_{ij} & d_{ij} \\ 0 & 0 & 0 & 1 \end{bmatrix} \tag{2} $$

The joint variables and parameters in Table I were engineered to produce the following matrices:

$$ {}^{0}A_{i1} = \begin{bmatrix} c\theta_{i1} & 0 & s\theta_{i1} & l_{i1}c\theta_{i1} \\ s\theta_{i1} & 0 & -c\theta_{i1} & l_{i1}s\theta_{i1} \\ 0 & 1 & 0 & 0 \\ 0 & 0 & 0 & 1 \end{bmatrix} \tag{3} $$

$$ {}^{1}A_{i2} = \begin{bmatrix} c\theta_{i2} & -s\theta_{i2} & 0 & l_{i2}c\theta_{i2} \\ s\theta_{i2} & c\theta_{i2} & 0 & l_{i2}s\theta_{i2} \\ 0 & 0 & 1 & 0 \\ 0 & 0 & 0 & 1 \end{bmatrix} \tag{4} $$

$$ {}^{2}A_{i3} = \begin{bmatrix} c\theta_{i3} & -s\theta_{i3} & 0 & l_{i3}c\theta_{i3} \\ s\theta_{i3} & c\theta_{i3} & 0 & l_{i3}s\theta_{i3} \\ 0 & 0 & 1 & 0 \\ 0 & 0 & 0 & 1 \end{bmatrix} \tag{5} $$

Equations (3)-(5) are substituted into equation (1) to acquire a motion equation related to foot i:

$$ {}^{0}T_{i3} = {}^{0}A_{i1}{}^{1}A_{i2}{}^{2}A_{i3} = \begin{bmatrix} n_X & o_X & a_X & P_X \\ n_Y & o_Y & a_Y & P_Y \\ n_Z & o_Z & a_Z & P_Z \\ 0 & 0 & 0 & 1 \end{bmatrix} \tag{6} $$

In equation form,

$$ P_X = c\theta_{i1}(c\theta_{i2}l_{i3}c\theta_{i3} - s\theta_{i2}l_{i3}s\theta_{i3} + l_{i2}c\theta_{i2}) + l_{i1}c\theta_{i1} $$
$$ P_Y = s\theta_{i1}(c\theta_{i2}l_{i3}c\theta_{i3} - s\theta_{i2}l_{i3}s\theta_{i3} + l_{i2}c\theta_{i2}) + l_{i1}s\theta_{i1} $$
$$ P_Z = s\theta_{i2}l_{i3}c\theta_{i3} + c\theta_{i2}l_{i3}s\theta_{i3} + l_{i2}s\theta_{i2} $$

2.2 Inverse kinematic analysis based on single-foot positive kinematic

In general, the position of the end of each foot is known and the angle of rotation of each joint must be found, so it is necessary to analyze the inverse kinematic of the feet.

The position of the end of foot i in root joint and foot coordinate systems $\{O_{i0} - X_{i0}Y_{i0}Z_{i0}\}$ and $\{O_{i3} - X_{i3}Y_{i3}Z_{i3}\}$ has the following transformation relation:

$$ \begin{bmatrix} {}^{0}x_{i3} \\ {}^{0}y_{i3} \\ {}^{0}z_{i3} \\ 1 \end{bmatrix} = {}^{0}T_{i3} \begin{bmatrix} {}^{3}x_{i3} \\ {}^{3}y_{i3} \\ {}^{3}z_{i3} \\ 1 \end{bmatrix} \tag{7} $$

where ${}^{0}x_{i3}, {}^{0}y_{i3}, {}^{0}z_{i3}$ is the position of the foot side in $\{O_{i0} - X_{i0}Y_{i0}Z_{i0}\}$, the root joint coordinate system; ${}^{3}x_{i3}, {}^{3}y_{i3}, {}^{3}z_{i3}$ is the position of the foot side in $\{O_{i3} - X_{i3}Y_{i3}Z_{i3}\}$, the foot side coordinate system; and the foot-side position is the original position of $\{O_{13} - X_{13}Y_{13}Z_{13}\}$:

$$ \begin{bmatrix} {}^{3}x_{i3} \\ {}^{3}y_{i3} \\ {}^{3}z_{i3} \\ 1 \end{bmatrix} = \begin{bmatrix} 0 \\ 0 \\ 0 \\ 1 \end{bmatrix} \tag{8} $$

Substituting equations (6) and (8) into equation (7), the corresponding matrix elements on both sides are equal to

$$ {}^{0}x_{i3} = c\theta_{i1}[l_{i3}c(\theta_{i2} + \theta_{i3}) + l_{i2}c\theta_{i2}] + l_{i1}c\theta_{i1} \tag{9} $$

$$ {}^{0}y_{i3} = s\theta_{i1}[l_{i3}c(\theta_{i2} + \theta_{i3}) + l_{i2}c\theta_{i2}] + l_{i1}s\theta_{i1} \tag{10} $$

$$ {}^{0}z_{i3} = l_{i3}s(\theta_{i2} + \theta_{i3}) + l_{i2}s\theta_{i2} \tag{11} $$

The following equation can be obtained by dividing equation (10) by equation (9):

$$ \theta_{i1} = \arctan\frac{{}^{0}y_{i3}}{{}^{0}x_{i3}} \tag{12} $$

Three equations can thus be obtained by equations (9)-(11):

$$ c\theta_{i1}[l_{i3}c(\theta_{i2} + \theta_{i3}) + l_{i2}c\theta_{i2}] = {}^{0}x_{i3} - l_{i1}c\theta_{i1} \tag{13} $$

$$ s\theta_{i1}[l_{i3}c(\theta_{i2} + \theta_{i3}) + l_{i2}c\theta_{i2}] = {}^{0}y_{i3} - l_{i1}s\theta_{i1} \tag{14} $$

$$ l_{i3}s(\theta_{i2} + \theta_{i3}) + l_{i2}s\theta_{i2} = {}^{0}z_{i3} \tag{15} $$

Set $x_i = {}^{0}x_{i3} - l_{i1}c\theta_{i1}$, $y_i = {}^{0}y_{i3} - l_{i1}s\theta_{i1}$, $z_i = {}^{0}z_{i3}$. Equations (13)-(15), calculated as $(13)^2 + (14)^2 + (15)^2$ are solved as follows:

$$ \theta_{i3} = -\arccos\left(\frac{z_i^2 + x_i^2 + y_i^2 - l_{i2}^2 - l_{i3}^2}{2l_{i2}l_{i3}}\right) \tag{16} $$

Similarly, calculating (15), $\frac{(15)}{\sqrt{(13)^2 + (14)^2}}$ gives equation (17):

$$ \theta_{i2} = \arctan\left(\frac{\frac{z_i}{\sqrt{x_i^2 + y_i^2}}(l_{i3}c\theta_{i3} + l_{i2}) - l_{i3}s\theta_{i3}}{\frac{z_i}{\sqrt{x_i^2 + y_i^2}}l_{i3}s\theta_{i3} + l_{i3}c\theta_{i3} + l_{i2}}\right) \tag{17} $$

The forward and inverse solutions obtained in this section provide a programming basis for the gait experiment of the robot behind. The forward solution of robot can predict the displacement and velocity of robot. The inverse solution of the robot provides the basis for the calculation of the rotation angle of each joint in different gait.

3. Gait comparisons

3.1 Analysis of the typical three-footed gait

The phase diagram of a hexapodal robot moving with a three-footed gait is displayed in Figure 2. When the robot moves with a three-footed gait, its six legs are divided into two groups, with feet 1, 3 and 5 in the first group and feet 2, 4 and 6 in the second. The feet in each group make up a triangle and bear the loading of the body to maintain its stability. During motion, the three feet in the same group are all in the swing (moving as a result of dangling) or supporting (touching the ground) phases simultaneously. The two groups of feet alternate with each other between the swing and supporting phases. If cycle T is when the when hexapod robot moves with a three-footed gait and every group of feet spends the same amount of time in the swing and supporting phases, the duty coefficient of every foot can be listed as:

$$ T_{swing} = T_{stance} = \frac{1}{2}T \tag{18} $$

$$ \varepsilon = \frac{T_{stance}}{T} = 1 - \frac{T_{swing}}{T} = \frac{1}{2} \tag{19} $$

Figure 2 Phase diagram of a three-footed gait

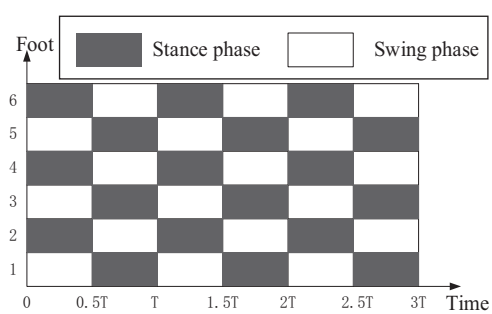

$T_{s\tan ce}$ in the above equation represents the time for which the foot remains supporting in this motion cycle; T_{swing} represents the time that a foot takes to keep itself in the swing phase; and ε is the duty coefficient – the proportion of how long this foot stays in stance phase in the whole cycle.

Assuming that the step size of the three-legged gait is p_1 and the exercise time is t_1, the number of steps required for the robot to advance by s distance is:

$$n_1 = \frac{s}{p_1} \tag{20}$$

The time spent in each step is:

$$t_{p_1} = \frac{t_1}{n_1} = \frac{t_1 \cdot p_1}{s} \tag{21}$$

The robot's average speed is:

$$\overline{v}_1 = \frac{s}{t_1} \tag{22}$$

Figure 3 shows a sketch of a three-footed gait by a hexapod robot, where a is the starting stance from a to b; feet 2, 4 and 6 stay in a swing situation; the hip joint controls the raising and lowering of feet and the root joint controls forward swaying of the feet. Feet 1, 3 and 5 still serve as support; the backswing of the root joints relies on foot-side friction to push the body forward. From b to c, feet 1, 3 and 5 remain in a swing phase and root joints drive the feet to swing forward. Feet 2, 4 and 6 are supports as the root joints swing back and rely foot-side friction to push the body forward. b and c are two typical situations during a three-footed gait: they work circularly to push the hexapod robot forward. d defines the termination stance for the hexapod robot during random occasions of b and c, causing the robot to stop walking.

As one of the robot's typical gaits, the three-footed gait has been applied extensively. As Figure 4 shows, the robot's body during rotation of root joints relies on foot-side friction to go forward; the supporting three feet can easily slide toward the robot, turning foot-side friction into sliding friction; moreover, coarse ground and foot-side forces exert major influences on sliding friction; the contingency of slide friction results in different degrees of foot-side sliding, causing deviations in the forward direction. When body of the robot moves forward, only the root joints rotate. The largest sliding volume from the foot side is described as follows:

Figure 3 Map of the three-footed gait

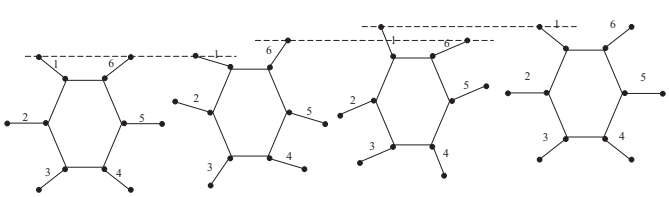

Notes: (a) Starting position-posture; (b) t = 0/t = T; (c) t = T/2; (d) End position-posture

$$\Delta d = \left(l_{i1} + \sqrt{2} l_{i2}/2\right)(1 - \cos\delta) \tag{23}$$

3.2 Four-footed propulsive gait based on kinematic analysis and planning

To solve the deflection problems of typical three-footed gaits from the rotation of the root joint, we propose a four-footed propulsive gait in which the front and back four root joints switch to planar positions in line with the forward direction and the robot cannot rotate its root joints; only two legs in the middle are used to stabilize the robot, as Figure 5 shows, so six legs are divided into the foreleg (1 and 6), midleg (2 and 5) and back leg (3 and 4). During movement, every group of legs retains the same pose.

The phase diagram of a four-footed propulsive gait is shown as Figure 6. If motion cycle of this gait is regarded as T, in this cycle, the gait could be divided into four phases; we stipulate that every phase should consume the same time and only one group of feet falls into the swing phase in this phase; therefore, the duty coefficient of the two feet in the midleg group can be described as follows:

$$T_{swing} = T_{\text{stance}} = \frac{1}{2} T \tag{24}$$

$$\varepsilon_{middle} = \frac{T_{\text{stance}}}{T} = 1 - \frac{T_{swing}}{T} = \frac{1}{2} \tag{25}$$

The duty coefficient of the four feet in the front and back front group can be listed as follows, respectively:

$$T_{swing} = \frac{1}{4} T,\ T_{\text{stance}} = \frac{3}{4} T \tag{26}$$

$$\varepsilon_{front} = \varepsilon_{back} = \frac{T_{\text{stance}}}{T} = 1 - \frac{T_{swing}}{T} = \frac{3}{4} \tag{27}$$

In the standing pose, in response to the 0, on this occasion in Figure 6, the tips of the front and back four feet should be in $(n_0\ 0\ m)$ in the coordinate system of the root joint. If $n_0 = 0.5\ (n_1 + n_2)$, the robot advances forward 0-0.25 T so that the mid-legs swing, and the forelegs maintain a stance like that in Figure 7(a). At this moment, the foot-side coordinate is $(n_1\ 0\ m)$, through which the robot's single-foot kinematic analysis is used to acquire:

$$\gamma_1 = -\arccos\left(\frac{m^2 + (n_1 - l_{i1})^2 - l_{i2}^2 - l_{i3}^2}{2 l_{i2} l_{i3}}\right) \tag{28}$$

$$\beta_1 = \arctan\left(\frac{\frac{m}{|n_1 - l_{i1}|}(l_{i3} c\gamma_1 + l_{i2}) - l_{i3} s\gamma_1}{\frac{m}{|n_1 - l_{i1}|} l_{i3} s\gamma_1 + l_{i3} c\gamma_1 + l_{i2}}\right) \tag{29}$$

The hindleg group moves as shown in Figure 7. For the second posture in a, when the coordinate of the end of the foot is $(n_2\ 0\ m)$, the kinematic analysis can be used to obtain the rotation angles of the joints of the foot:

Figure 4 Sketch of the side of the foot slide during forward propulsion of the robot's body

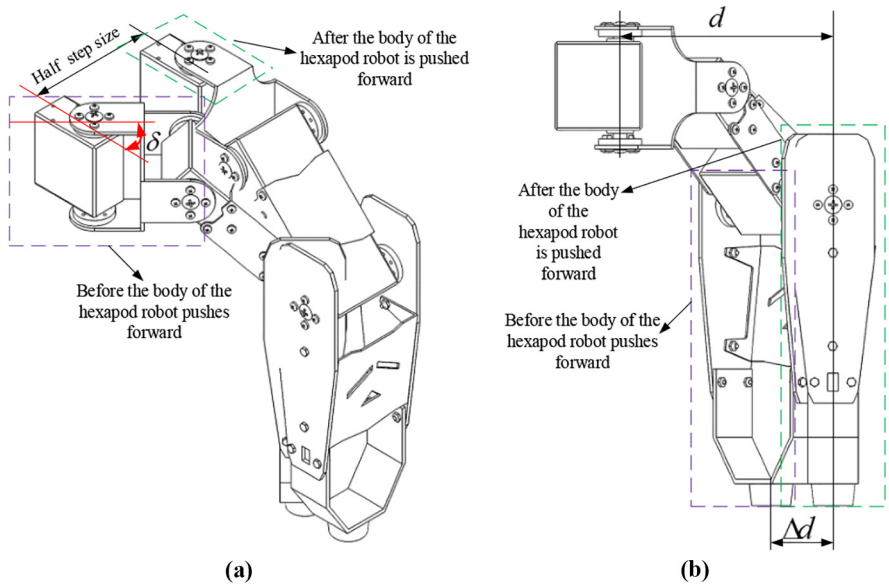

Notes: (a) Axonometric view; (b) main view

Figure 5 Foot position distribution for a four-footed propulsive gait

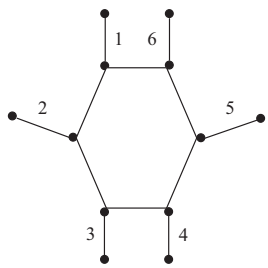

Figure 6 Phase diagram of the four-footed propulsive gait

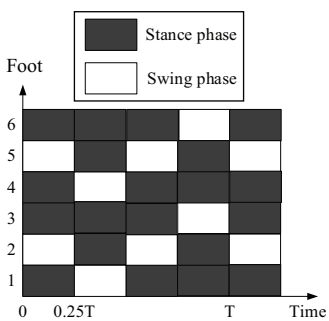

$$\gamma_2 = -\arccos\left(\frac{m^2 + (n_2 - l_{i1})^2 - l_{i2}^2 - l_{i3}^2}{2l_{i2}l_{i3}}\right) \tag{30}$$

$$\beta_2 = \arctan\left(\frac{\frac{m}{|n_2 - l_{i1}|}(l_{i3}c\gamma_2 + l_{i2}) - l_{i3}s\gamma_2}{\frac{m}{|n_2 - l_{i1}|}l_{i3}s\gamma_2 + l_{i3}c\gamma_2 + l_{i2}}\right) \tag{31}$$

Figure 7 Sketch of two poses of a foot in the four-footed propulsive gait

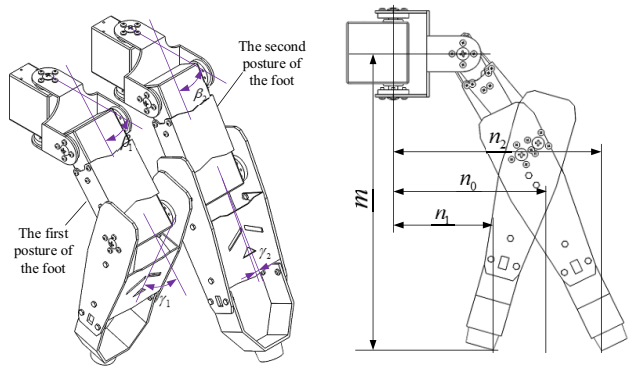

Note: (a) Axonometric view; (b) main view

The body moves a distance of $0.5(n_2 - n_1)$; at times 0.25 T-0.5 T, the back leg group is swung to the first posture by the stable supporting action of the midleg group; during 0.5 T-0.75 T, the midleg group swings to the front position of the middle portion of the robot, stabilizing the support for the swing of the next foreleg group; during 0.75 T-T, the foreleg group swings to the second posture. In the next cycle, when the midleg group is in the backward swing state, the front and rear foot joints rotate to push the body forward. After this advancement, the foreleg group is again in the first posture; the rear foot groups are in the second posture; and the advancement distance is $(n_2 - n_1)$. The front and rear foot cycles are in the first and second postures, pushing the robot forward.

Assuming that the step distance of the four-legged gait is p_2 and the movement time is t_2, the number of steps required for the robot to advance by s distance is:

$$n_2 = \frac{s}{p_2} \tag{32}$$

The time spent in each step is:

$$t_{p_2} = \frac{t_2}{n_2} = \frac{t_2 \cdot p_2}{s} \tag{33}$$

The average speed of robot motion is:

$$\overline{v}_2 = \frac{s}{t_2} \tag{34}$$

Comparing the duty coefficient, the four-footed propulsive gait has higher stability.

4. Experimental verification

We used the hexapod robot shown in Figure 8 in verification experiments to prove whether a four-footed gait could solve the walking deviation exhibited in a typical three-footed gait. The joints of the robot are meshed by the adjusted gears to ensure that there is no virtual displacement when the robot is walking. Each joint of the robot is driven by an LDX-218 digital actuator, to acquire concrete data of the robot's motion and for convenient comparison and analysis; one JY901 attitude sensor placed on the robot's body is used to detect the robot's deflection angle during motion and transfers data through a wireless serial port module to the computer for recording. Its angular accuracy is 0.001 degree, and its angular velocity accuracy is 0.0001 degree/s. A block diagram of data collection is shown as Figure 9. In an experimental environment containing a 1-m flat cement floor, we compare the robot's two gaits, compare experimental data and, finally, analyze the outcomes.

4.1 Typical three-footed gait experiment

When the robot moves in a typical tripod gait after several experiments p_1 = 86 mm, three groups of experiments can be carried out according to equations (20)-(22) and t_1 = 30 s, 1 min and 2 min. The corresponding average speed of the robot is shown in Table II.

Figure 8 The hexapod robot used in experiments

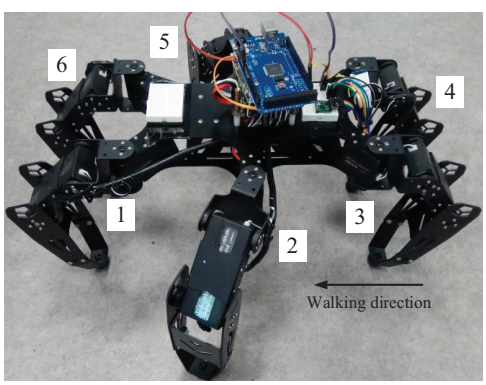

Figure 9 Block diagram of data collection

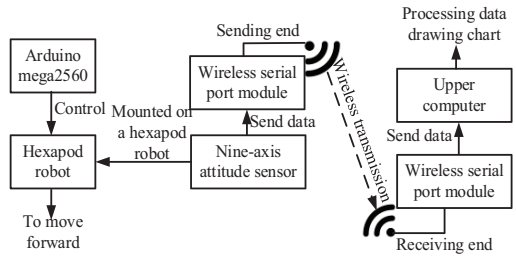

To display the contingency of foot-side friction, every group of experiments is carried out four times; the experimental results are as shown in Figure 10.

The experimental results in Figure 10 show the following:

- In *a*, when the hexapod robot moves forward 1 m, the directional deviation is within 10°−20°. Every step is troubled by swaying and the uncertainty of foot-side friction leads to positive and negative deviation, so the deflection angle of the four-time experiment varied; as time passes, the directional deviation of the robot's motion increases gradually.
- In *b*, when the hexapod robot moves forward 1 m, the directional deviation stays within 5°−30° and the uncertainty of foot-side friction also faces positive and negative deviation. Further, there is one big gap in the deflection angle in every experiment, which gradually increases over time.
- In *c*, when the hexapod robot moves forward 1 m, directional deviation is 5°−35°. The uncertainty of foot-side friction also faced with negative deviation; moreover, there is a large gap in the deflection angle in every experiment. As time passes, the directional deviation of the robot's motion increases gradually.

4.2 Four-foot propulsive gait experiment

After several experiments p_2 = 85 mm, the robot has four-feet propulsion gait motion. Therefore, according to equations (32)-(34) and t_2 = 1 min, 2 min and 3 min, we can conduct three sets of experiments separately. The average speed of the robot is as shown in Table III.

Every group of experiments was carried out four times; the experimental results are shown in Figure 11.

In Figure 11, the experimental results show the following:

- In *a*, when the hexapod robot moves forward 1 m, the directional deviation is kept to 0°−1.4°, causing a minor sway; the existing directional deviation in four experimental situations increases and then decreases.

Table II Experimental parameters of three-foot gait

s (mm)	p_1 (mm)	n_1 (step)	t_1 (s)	t_{p_1} (s)	$\overline{v}_1$ (mm/s)
1,000	86	12	30	2.5	33.3
			60	5.0	16.7
			120	10.0	8.3

Figure 10 Angle deflection on the hexapod robot moving forward 1 m with a typical three-foot gait

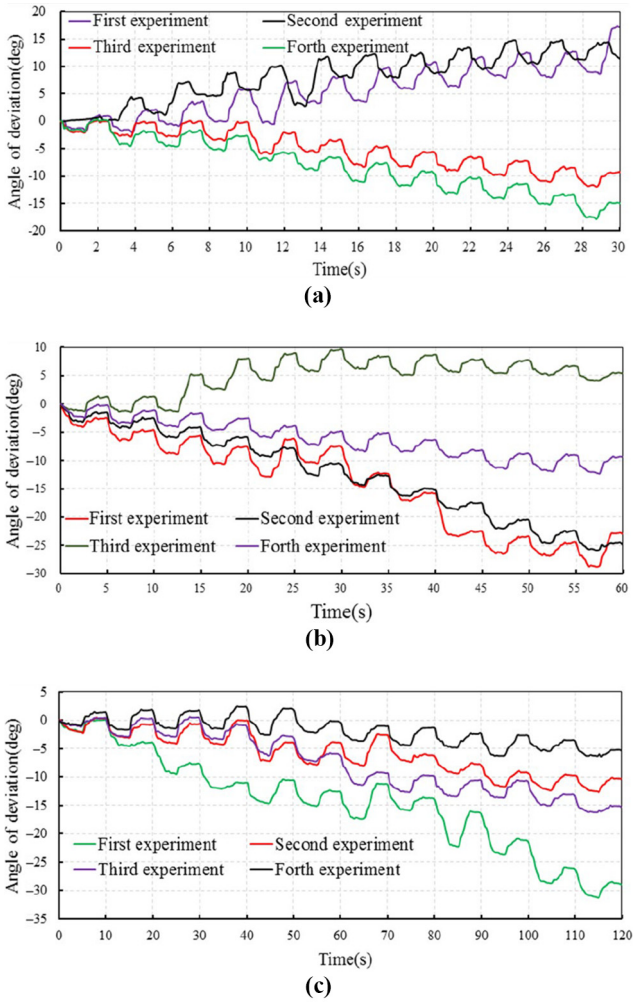

Note: (a) Forward motion lasts 30 s; (b) forward motion lasts one minute; (c) the forward motion lasts two minutes

Figure 11 Angle deflection of the hexapod robot moving forward 1 m with the four-footed propulsive gait

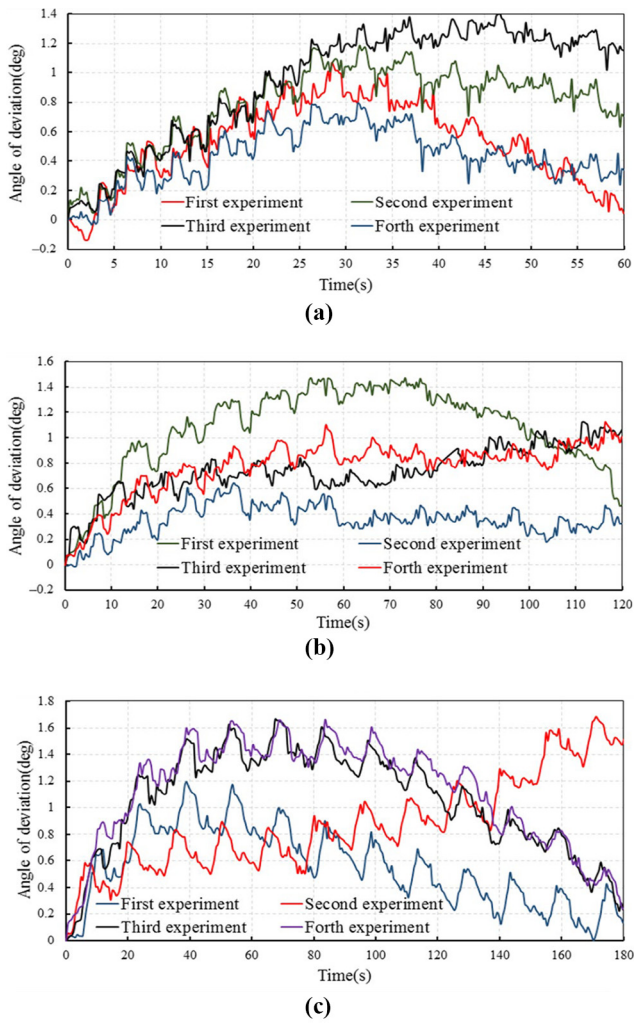

Notes: (a) Forward motion lasts 1 min; (b) forward motion lasts 2 min; (c) forward motion lasts 3 min

- In *b*, when the hexapod robot moves forward 1 m, the directional deviation is kept to within 0°−1.6° and motion shows a minor sway. There is a smaller gap in the existing directional deviation in the experiments.
- In *c*, when the hexapod robot moves forward 1 m, the directional deviation stays within 0°−1.8° and every step exhibits a swing. The directional deviation in the second experiment increased over time and the deviation in the three other experiments first increased and then decreased.

Table III Experimental parameters of quadruped gait

s (mm)	p_2 (mm)	n_2 (step)	t_2 (s)	t_{p_2} (s)	$\overline{v}_2$ (mm/s)
1,000	85	12	60	5.0	16.7
			120	10.0	8.3
			180	15.0	5.6

5. Conclusions

This study investigated the deviations that a hexapod robot might experience in a typical three-foot gait motion, analyzes the real reasons of would-be deviation and combine kinematic analysis of multi-freedom manipulators to plan four-foot propulsive gait; the comparative experiment of two gaits can be summarized as follows:

- In identical experimental environments, hexapodal robots experience smaller deviations when using a four-footed propulsive gait from a typical three-footed gait for forward motion.
- For the same distance but at different speeds, the deviation basically keeps itself within the same range when the robot advances forward with a four-foot propulsive gait.
- Because the foot slide in the three-footed gait sometimes experiences frictions, the robot exhibits a

large gap in directional deviations in different courses during motion.

- For motion using a four-footed propulsive gait, there are minor directional deviations of hexapodal robots resulting from experimental errors, which can be reduced through optimizing mechanical structures.

Planning different gaits can solve problems existing in some typical gaits. This article has put forward a gait planning method for hexapodal robots moving forward with diverse gaits as a redundant multifreedom structure. Subsequent research can combine a multiparallel-legged structure to perform kinematic analysis, optimize the robot's mechanical structure and carry out in-depth research on hexapod robot gaits.

References

Abhijit, M., Shekhar, R.S. and Kumar, P. (2018), "Study on feet forces' distributions, energy consumption and dynamic stability measure of hexapod robot during crab walking", *Applied Mathematical Modelling*, Vol. 65 No. 11, pp. 717-744.

Agheli, M. and Nestinger, S.S. (2016), *Foot Force Based Reactive Stability of Multi-Legged Robots to External Perturbations*, Kluwer Academic.

Arevalo, J., Sanz-MerodioC. and Garcia, D. (2014), "E.: reactive humanoid walking algorithm for occluded terrain", *Proceedings of the First Iberian Robotics Conference*, New York, NY, pp. 397-410.

Armada, M., Prieto, M., Akinfiev, T., *et al.* (2005), "On the design and development of climbing and walking robots for the Maritime industries", *Journal of Maritime Research*, Vol. 11 No. 1, pp. 9-32.

Castro, X.Y.S. and Castaneda, E.C. (2019), "Terrain Adaptability Strategies Statically-Stable for a Walking Hexapod Robot", *Revista Iberoamericana De Automatica E Informatica Industrial*, Vol. 16 No. 3, pp. 332-343.

Chen, G., Jin, B. and Chen, Y. (2014), "Solving position-posture deviation problem of multi-legged walking robots with semi-round rigid feet by closed-loop control", *Journal of Central South University*, Vol. 21 No. 11, pp. 4133-4141.

Ding, K. (2016), *Research on Biped Locomotion Gait Planning and Control System for Six Legged Robot*, Southeast University.

Fujita, T. and Tsuchiya, Y. (2015), "Development of a tracked mobile robot equipped with two arms", *Industrial Electronics Society, IECON Conference of the IEEE*, IEEE, pp. 2738-2743.

Gao, H., Jin, M., Liu, Y., *et al.*, (2015), "Turning gait planning and simulation validation of a hydraulic hexapod robot", *International Conference on Fluid Power and Mechatronics*, IEEE, pp. 842-847.

Gonzalez de Santos, P., Garcia, E., Ponticelli, R., *et al.*, (2009), "Minimizing energy consumption in hexapod robots", *Advanced Robotics*, Vol. 23 No. 6, pp. 681-704.

Grand, C., Amar, F.B., Plumet, F., *et al.*, (2004), "Stability and traction optimization of a reconfigurable Wheel-Legged robot", *The International Journal of Robotics Research*, Vol. 23 No. 10-11, pp. 1041-1058. Vol No

Grieco, J.C., Prieto, M., Armada, M., *et al.*, (1998), "Six-Legged climbing robot for high payloads", *6th IEEE Conference on Control Applications ICCA'98. Trieste*, pp. 1-4.

Grzelczyk, D., Stanczyk, B. and Awrejcewicz, J. (2017), "Kinematic, dynamics and power consumption analysis of the hexapod robot during walking with Tripod Gait", *International Journal of Structural Stability & Dynamics*, Vol. 17 No. 5, pp. 1740-1750.

Guardabrazo, T.A. and Gonzalez de Santos, P. (2004), "Building an energetic model to evaluate and optimize power consumption in walking robots", *Industrial Robot: An International Journal* , Vol. 31 No. 2, pp. 201-208.

Hasnaa, E.H. and Mohammed, B. (2017), "Planning tripod gait of an hexapod robot", *International Multi-Conference on Systems, Signals & Devices*. New York, NY, pp. 163-168.

Lee, C.H., Kim, S.H. and Kang, S.C. (2003), "Double-track mobile robot for hazardous environment applications", *Advanced Robotics*, Vol. 17 No. 5, pp. 447-459.

Li, J., Sun, Y. and Wu, H. (2017), "Review of gait analysis and planning of legged robot", *International Conference on Management, Education, Information and Control*, pp. 278-283.

Montes, H., Mena, L., Fernández, R., *et al.*, (2017), "Energy-efficiency hexapod walking robot for humanitarian demining", *Industrial Robot: An International Journal*, Vol. 44 No. 4, pp. 457-466.

Song, Z., Ren, H., Zhang, J. and Ge, S.S. (2016), "Kinematic analysis and motion control of wheeled mobile robots in cylindrical workspaces", *IEEE Transactions on Automation Science and Engineering*, Vol. 13 No. 2, pp. 1207-1214.

Sun, Q., Gao, F. and Chen, X.B. (2018), "Towards dynamic alternating tripod trotting of a pony-sized hexapod robot for disaster rescuing based on multi-modal impedance control", *Robotica*, Vol. 36 No. 7, pp. 1048-1076.

Yang, P. and Feng, G. (2014), "A new six-parallel-legged walking robot for drilling holes on the fuselage", *Proceedings of the Institution of Mechanical Engineers Part C Journal of Mechanical Engineering Science*, Vol. 228 No. 4, pp. 753-764.

Yin, X.L. (2014), *Gait Planning and Control Strategy of Six Legged Bionic Robot*, Harbin Institute of Technology.

Zhang, C., Jiang, X., Teng, M., *et al.*, (2016), "Research on gait planning and static stability of hexapod walking robot", *International Symposium on Computational Intelligence and Design*. IEEE, pp. 176-179.

Zhao, Y., Chai, X., Gao, F., *et al.*, (2018), "Obstacle avoidance and motion planning scheme for a hexapod robot Octopus-III", *Robotics & Autonomous Systems*, Vol. 31 No. 5, pp. 412-420.

Zhong, G., Chen, L. and Deng, H. (2017), "A performance oriented novel design of hexapod robots", *IEEE/ASME Transactions on Mechatronics*, Vol. 22 No. 3, pp. 1435-1443.

Zhong, G., Chen, L., Jiao, Z., *et al.*, (2017), "Locomotion control and gait planning of a novel hexapod robot using biomimetic neurons", *IEEE Transactions on Control Systems Technology*, Vol. 99 No. 12, pp. 1-13.

Zhong, G., Chen, L., Jiao, Z., *et al.*, (2018), "Locomotion control and gait planning of a novel hexapod robot using biomimetic neurons", *IEEE Transactions on Control Systems Technology*, Vol. 36 No. 2, pp. 624-636.

Zhong, G., Deng, H., Xin, G., *et al.*, (2016)"Dynamic hybrid control of a hexapod walking robot: experimental verification", *IEEE Transactions on Industrial Electronics*, Vol. 63 No. 8, pp. 5001-5011. No

Zhu, Y., Guo, T., Liu, Q., *et al.*, (2017), "Turning and radius deviation correction for a hexapod walking robot based on an Ant-Inspired sensory strategy", *Sensors*, Vol. 17 No. 12, pp. 2710-2715.

Zhu, Y.G., Guo, T., Liu, Q., *et al.*, (2017), "A study of arbitrary gait pattern generation for turning of a bio-inspired hexapod robot", *Robotics and Autonomous Systems*, Vol. 97 No. 12, pp. 125-135.

Zhuang, H.C., Gao, H.B. and Deng, Z.Q. (2017), "Gait planning research for an electrically driven Large-Load-Ratio Six-Legged robot", *Applied Sciences*, Vol. 7 No. 3, pp. 296-305.

About the authors

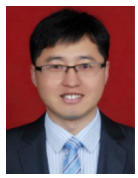

Zijie Niu was born in Baoji, Shaanxi Province of China, in 1985. He graduated from the Nanjing University of Aeronautics and Astronautics, and obtained a doctor's degree in engineering. The main research areas are robot and its design control, and ultrasonic motor design and drive. Zijie Niu is the corresponding author and can be contacted at: niuzijie@nwsuaf.edu.cn

Aiwen Zhan was born in Jiujiang, Jiangxi Province of China, 1995. He is a postgraduate student from the South China University of Technology. The main research areas are robot and its design control.

Yongjie Cui was born in Suihua, Heilongjiang Province of China, 1971. He is a Professor at Northwest Agriculture and Forestry University. The main research areas are robot and end effector.